The magnetic field topology associated with two M flares

M.L. Luoni [a,*], C.H. Mandrini [a,1], G.D. Cristiani [a], P. Démoulin [b]

[a] *Instituto de Astronomía y Física del Espacio, CONICET-UBA, CC. 67 Suc. 28, 1428 Buenos Aires, Argentina*
[b] *Laboratoire d'Etudes Spatiales et d'Instrumentation en Astrophysique (LESIA), Observatoire de Paris, 5 place Jules Janssen, F-92195 Meudon, Cedex, France*

Abstract

On 27 October, 2003, two GOES M-class flares occurred in an interval of 3 h in active region NOAA 10486. The two flares were confined and their associated brightenings appeared at the same location, displaying a very similar shape both at the chromospheric and coronal levels. We focus on the analysis of magnetic field (SOHO/MDI), chromospheric (HASTA, Kanzelhöhe Solar Observatory, TRACE) and coronal (TRACE) observations. By combining our data analysis with a model of the coronal magnetic field, we compute the magnetic field topology associated with the two M flares. We find that both events can be explained in terms of a localized magnetic reconnection process occurring at a coronal magnetic null point. This null point is also present at the same location one day later, on 28 October, 2003. Magnetic energy release at this null point was proposed as the origin of a localized event that occurred independently with a large X17 flare on 28 October, 2003 [Mandrini, C.H., Démoulin, P., Schmieder, B., Deluca, E., Pariat, E., Uddin, W. Companion event and precursor of the X17 flare on 28 October, 2003. Solar Physics, 238, 293–312, 2006], at 11:01 UT. The three events, those on 27 October and the one on 28 October, are homologous. Our results show that coronal null points can be stable topological structures where energy release via magnetic reconnection can happen, as proposed by classical magnetic reconnection models.
© 2007 COSPAR. Published by Elsevier Ltd. All rights reserved.

Keywords: MHD and plasmas; Solar Physics; Magnetic reconnection; Flares

1. Introduction

Activity in the solar corona, such as flares, coronal mass ejections and, at a low energy-release level, coronal heating, is thought to be related to the way in which the coronal field reacts to sub-photospheric motions. However, the efficiency with which the field produces energetic events depends on the degree of its complexity. That is to say, on the presence of topological structures such as null points, separators, separatrices and quasi-separatrix layers, which provide the small scales where magnetic reconnection can efficiently occur (see the recent reviews by Démoulin, 2005, 2006; Longcope, 2005).

The first models of magnetic reconnection were developed in 2D (dimensions) (Parker, 1957; Sweet, 1958). In these models magnetic reconnection occurs at locations where the two components of the field vanish, which are called X points. When these models are extended to 3D, keeping invariance by translation, the X point becomes a null line, which is structurally unstable (when breaking the translation invariance). The generalization to 3D of a 2D null point is simply a point where the three components of the field vanish. Contrary to null lines, these are in general structurally stable. Coronal null points have been found in few observational examples, either associated with solar flares (see e.g. Mandrini et al., 1991, 1993; Gaizauskas et al., 1998; Longcope and Silva, 1998; Fletcher et al., 2001; Longcope et al., 2005; Mandrini et al., 2006) or with precursors to coronal mass ejections (see e.g. Aulanier et al., 2000; Gary and Moore, 2004), as proposed by the breakout model

* Corresponding author. Tel.: +54 11 4551 6035.
 E-mail address: mluoni@iafe.uba.ar (M.L. Luoni).
[1] Member of the Carrera del Investigador Científico, CONICET, Argentina.

for CMEs (Antiochos et al., 1999). However, when they are searched for in a systematic way, they do not appear to be common features (Démoulin et al., 1994).

The spectacular level of activity displayed by the Sun from 19 October until 4 November, 2003, originated from three β–γ–δ sunspot groups (NOAA 10484, 10486, 10488). Eight of the twelve X-flares, observed during this period, started in active region (AR) 10486. This unusually strong activity has been investigated in special issues of the Journal of Geophysical Research, Geophysical Research Letters and Space Weather published in 2004 and 2005 (see: http://www.agu.org/journals/ss/VIOLCONN1/). AR 10486 was also the site of other minor events (lower class) during that period. In particular, two M flares occurred on 27 October in an interval of 3 h. The first flare started in soft X-rays at 09:21 UT and was classified as an M5.0. It appeared as an impulsive peak during the decay phase of a previous flare that occurred in AR 10484. The second flare, homologous to the first one, started at 12:27 UT and was classified as an M6.7. Both events are indicated by arrows in Fig. 1.

In this paper, we concentrate in the analysis and interpretation of the two M flares. We combine data analysis with magnetic field modeling, which allows us to study the topology of the field at the location of the flares and propose a probable scenario for their origin. In Section 2, we describe the observations; while in Section 3, we present our magnetic field model and topology analysis. Finally, in Section 4, we show that the field topological structure is similar to that found by Mandrini et al. (2006) to explain the origin of the localized event that accompanied the two-ribbon X17 flare observed on 28 October, 2003, in the same AR. We discuss our results in the context of magnetic reconnection theory. Preliminary results of this study have been presented elsewhere (Luoni et al., 2005).
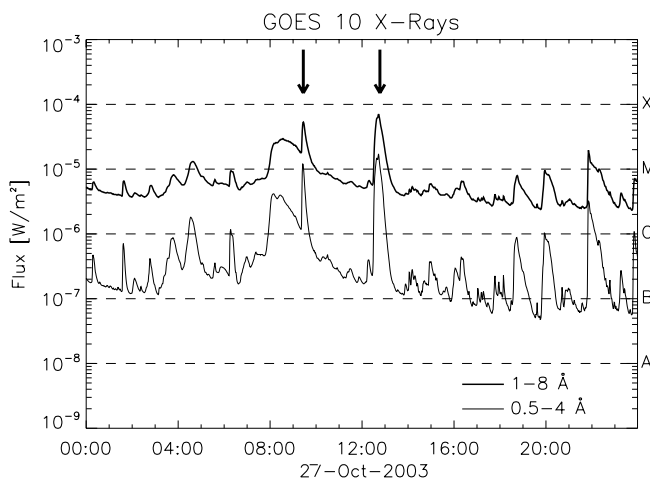
2. Observational characteristics of the events

2.1. Instruments and data

In this paper, we use full-disk level 1.5 magnetic maps from the Michelson Doppler Imager (MDI, Scherrer et al., 1995) aboard the Solar and Heliospheric Observatory (SOHO). These are the average of five magnetograms taken with a cadence of 30 s. The maps are constructed once every 96 min. The error in the flux densities per pixel in the averaged magnetograms is about ± 9 G, and each pixel has a mean area of 2.08 Mm^2.

To obtain the complete temporal coverage of both flares, we use Hα observations from the Kanzelhöhe Solar Observatory for the flare in the morning, and from the Hα Solar Telescope for Argentina (HASTA, see Fernández Borda et al., 2002) for the flare at noon on 27 October. Both telescopes, Kanzelhöhe and HASTA, provide full-disk images with a pixel size of 1.09 arcsec and 2.07 arcsec, respectively.

Transition region and coronal observations, and also chromospheric data, come from the Transition Region and Coronal Explorer (TRACE, Handy et al., 1999). TRACE was observing with high temporal cadence (60 s) in the 1600 Å and 195 Å passbands with a FOV of 768 arcsec × 768 arcsec at the times of both flares. The pixel size in all images is 0.5 arcsec, giving a spatial resolution of 1.0 arcsec.

The plasma observed by TRACE in the 1600 Å bandpass has temperatures in the range of $4–10 \times 10^3$ K (Handy et al., 1999, their Table I), temperatures that correspond to the upper photosphere and chromosphere. As the spots are clearly visible in these images, they have been used to coalign TRACE images with magnetic and chromospheric data.

2.2. The magnetic field evolution

AR 10486 arrived at the east solar limb on 23 October, 2003, with an already complex magnetic configuration. A detailed description of the AR magnetic field evolution can be found in Mandrini et al. (2006). We describe only what is meaningful to understand the flares discussed in this paper. Fig. 2 shows the AR configuration on 26 and 27 October, 2003. All polarities in this figure have been numbered as in Mandrini et al. (2006, their Fig. 2) for comparison. Polarities 3 and 4 in Fig. 2 (left) emerged when the AR was still on the far side of the Sun. This emergence occurred within a mainly negative field environment (to which polarity 1 belonged). The leading polarity 3 was located very close to the trailing positive polarity of an already decayed AR (polarity 2). To the north of the positive polarity 4, several bipoles emerged. Polarities 5 and 6 in Fig. 2 (right), which continued growing as the AR approached the central meridian passage, were already present at the east limb. On 25 October a very small bipole (polarities 7 and 8 in Fig. 2, right; see also the small bipole

Fig. 1. GOES light curve for 27 October, 2003. The two analyzed flares are pointed at by arrows.
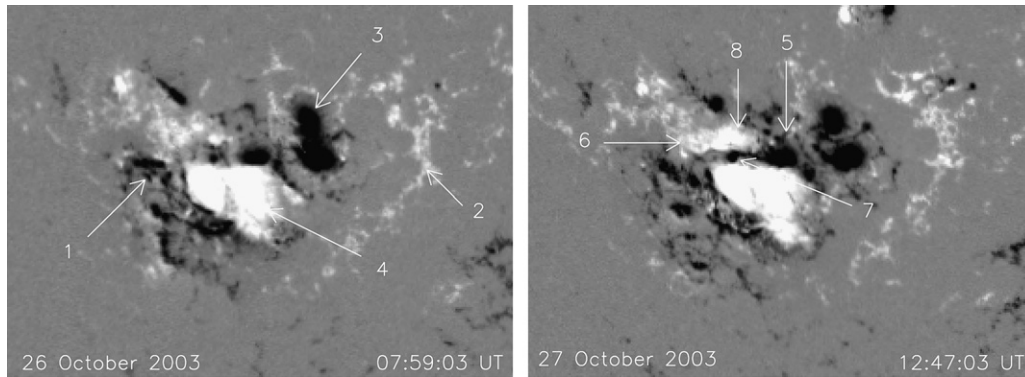
Fig. 2. MDI maps showing the magnetic configuration in AR 10486 on 26 and 27 October, 2003. The polarities that are involved in the two M flares discussed in this paper are marked as 4, 5, 7 and 8. Other polarities present in the AR have been numbered as described in Section 2.2. The area covered by the images is 271 × 201 pixels (536 arcsec × 398 arcsec). The magnetic field values have been saturated above (below) 500 G (−500 G). Positive (negative) field values are shown in white (black). In this and all the figures depicting the observations, solar north is to the top and west is to the right.

at the north of polarity 4 in the left panel) started to emerge. By 26 October it was clearly above the main inversion line. This field emergence created a positive region (merging of 6 and 8) separated from the main positive spots (polarity 4) by an elongated negative zone (merging of 5 and 7).

2.3. The events at chromospheric level

The flare during the morning of 27 October appears in Kanzelhöhe images as four separated kernels or ribbons (see Fig. 3, left). They are located over polarities 4, 5, 7 and 8. These brightenings appear, increase in intensity and decay at the same place all along the flare duration; the absence of observed ejecta at the flare location and the Hα kernel evolution indicates that the event is confined. Two of these ribbons are smaller and more compact, those over polarities 4 and 8; while the ones over 7 and 5 are more elongated and they even merge in this case. In particular, the kernel over polarity 7 lies also partially over polarity 8; errors in the coalignment between Hα and magnetic

maps, that we estimate as ±1 chromospheric image pixel, can be at the origin of this overlapping. The behaviour displayed by the Hα observations is also seen in TRACE 1600 Å images. An overlay between a TRACE image in this band, at the same time as the Kanzelhöhe image, and the closest in time MDI magnetic map can be seen in the left panel of Fig. 4.

Concerning the flare on 27 October at noon, it displays an extremely similar behavior as the flare in the morning, both in Hα and 1600 Å meaning that these two M flares are homologous. An image from the HASTA telescope is shown in the right panel of Fig. 3, while a TRACE image at the same time in 1600 Å band is shown in the right panel of Fig. 4.

We denoted the ribbons of both flares using the letter "r" for ribbon and the number corresponding to the polarity over which the brightening lies. This is the same way as used by Mandrini et al. (2006) in their Figures 2 and 3 to denote the brightenings associated with the small event that accompanied the two-ribbon X17 flare. During the flares on 27 October the main active region filament was seen
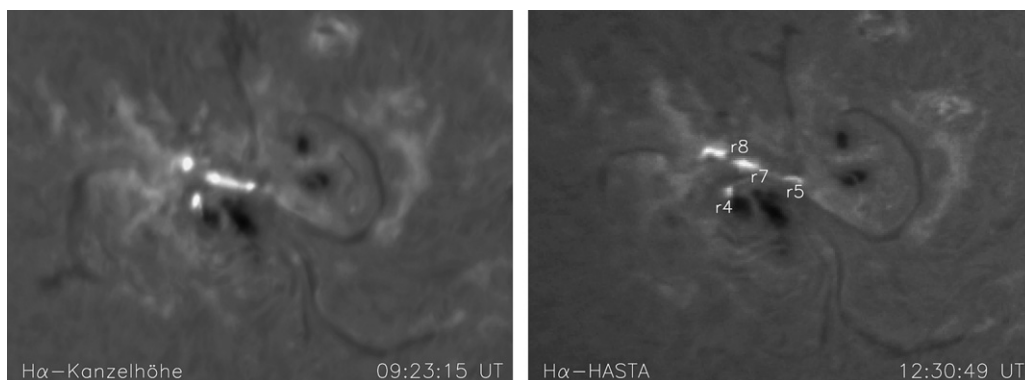

Fig. 3. The two M flares in Hα. The left panel shows an image of the first flare starting at 09:21 UT from Kanzelhöhe Solar Observatory, while the image on the right is an HASTA image of the second flare starting at 12:27 UT. The field of view in these images is the same as shown in Fig. 2. The area covered by the left image is 491 × 364 pixels, while for the right image it is 259 × 192 pixels (536 arcsec × 398 arcsec). Notice the similitude between the locations and shapes of the flare kernels. The flare ribbons have been marked in the right image, as discussed in the text.
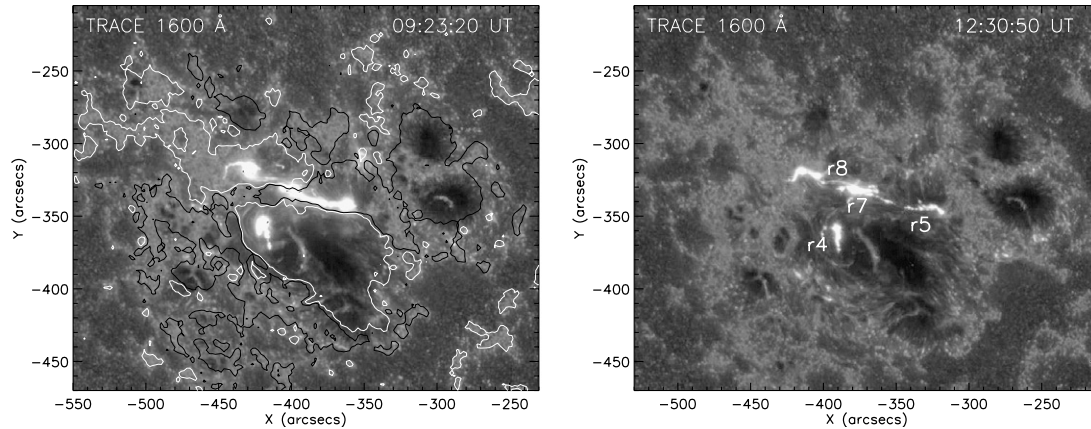
Fig. 4. TRACE images in 1600 Å showing the locations of the brightenings of both M flares. Notice the similitude in the shapes and locations of both flare ribbons. An MDI (magnetogram at 9:35 UT) isocontour of ±100 G (white/black continuous line corresponds to the positive/negative field value) has been overlaid on the image on the left, while on the image on the right we have numbered the flare ribbons as discussed in the text. The field of view is the same in both panels.

to activate (its plasma was probably heated), but it did not erupt; its eruption occurred on the next day followed by the large two-ribbon flare.

2.4. The events at coronal level

Bright coronal emission was observed by TRACE in 195 Å in the neighborhood of polarities 7 and 8 for both M flares. In both cases, these brightenings had the shape of curved loops and extend above the inversion lines separating the negative elongated region from the positive polarities northward and southward (Fig. 5). These loops are associated with the four ribbons (r4, r5, r7, r8) shown in Figs. 3 and 4. This is what we expect in case of confined quadrupolar reconnection, i.e. each pair of ribbons is associated with a set of reconnected field lines. These loop brightenings appear, grow in intensity and fade at the same location and keeping approximately the same shape during both flares.

3. The origin of the homologus M flares

3.1. The coronal-field model

To understand the origin of the emission described in the previous sections, we study its relationship to the 3D AR magnetic structure. To do so, we model the AR coronal field extrapolating the observed line of sight magnetic field under the linear force-free field assumption ($\vec{\nabla} \times \vec{B} = \alpha \vec{B}$, with α constant). We follow the method described in Démoulin et al. (1997), which is based on a fast Fourier transform as proposed by Alissandrakis (1981). This model takes into account the transformation of coordinates from the AR location to disk center. We have taken as boundary condition the MDI magnetogram in between the two M flares, at 11:11 UT on 27 October, 2003.

The only free parameter in our model is α. We determine its value by best fitting the loops observed by TRACE in
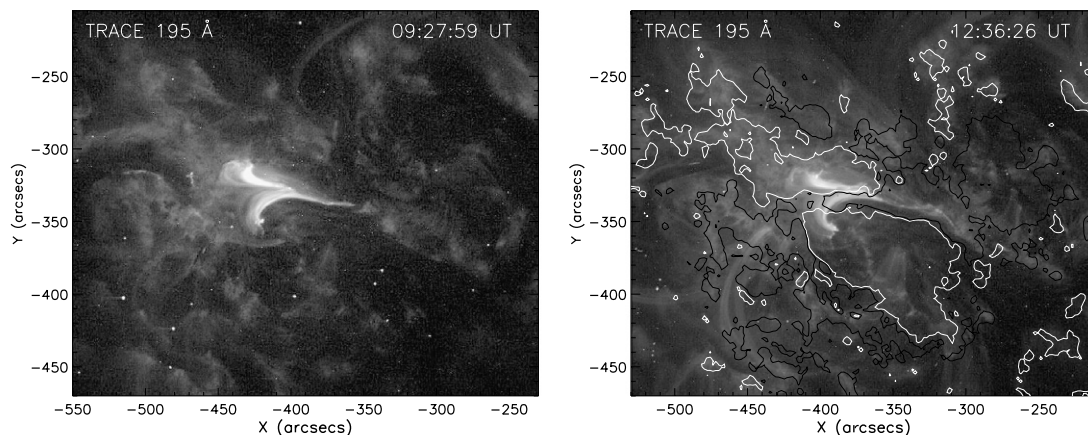

Fig. 5. TRACE images in 195 Å showing the flare loop brightenings at coronal level of both M flares. Notice the similarity in the locations and shapes of the flares. An MDI (magnetogram at 12:47 UT) isocontour of ±100 G (white/black continuous line corresponds to the positive/negative field value) has been overlaid on the image on the right as a reference. The field of view is the same in both panels.

195 Å (see Section 3.2 and Figs. 5 and 7). The magnetic field in AR 10486 is highly non-potential (Zhang et al., 2003) and, therefore, the α value that gives the best match to TRACE loops turned out to be the largest possible allowed by our model for the size of our integration box, $\alpha = -3.1 \times 10^{-2}\,\text{Mm}^{-1}$. The chosen box includes all the relevant AR polarities and is large enough to avoid aliasing effects (see e.g. Mandrini et al., 1996; Démoulin et al., 1997; Green et al., 2002).

As shown in the right panel of Fig. 7, our computed field lines follow quite well the shape of TRACE loops in Fig. 5, even so they do not reach as far to the east where ribbon r8 lies. Our model is limited in the sense that our value of α is the same for all points at the photosphere. However, as discussed below, the same topology was found for this AR at the locations of the flares using a non-linear force-free field extrapolation by (Régnier and Fleck, 2004). Since the magnetic configuration is locally quadrupolar (polarities 4, 5, 7 and 8), the magnetic topology is strongly defined by the magnetic flux distribution at the photospheric level; the magnetic field created by the coronal electric currents only deforms this topology.

3.2. The coronal-field topology

We explore the coronal magnetic field configuration in search of topological structures that can be associated to the observed flare ribbons and loops. We find the presence of a 3D magnetic null point located at a height of 3.1 Mm above the magnetogram, over the elongated negative polarity (polarity 7). The location of the null is shown in the left panel of Fig. 6. The vicinity of a null point can be described by the linear term in the local Taylor expansion of the magnetic field. By diagonalizing the Jacobian matrix of the field, we can find three orthogonal eigenvectors describing the structure of the field in the null neighborhood (Molodenskii and Syrovatskii, 1977). The divergence-free condition imposes that the sum of the three corresponding eigenvalues vanishes ($\lambda_1 + \lambda_2 + \lambda_3 = 0$). Furthermore, if the magnetic field is in equilibrium with the plasma ($\vec{j} \times \vec{B} = \vec{\nabla}P$), the eigenvalues are real (Lau and Finn, 1990). This means that two eigenvalues, say λ_1, λ_2, have the same sign, which is opposite to that of the third eigenvalue (λ_3). The two field lines that start at an infinitesimal distance from the null, in directions parallel and antiparallel to the eigenvector associated with λ_3, are called the two spines of the null. All field lines starting at an infinitesimal distance from the null in the plane defined by the two eigenvectors associated with λ_1 and λ_2, define what is called the fan surface. Further information on magnetic nulls can be found in Greene (1988); Lau (1993); Longcope et al. (2005)).

The magnetic null point found in AR 10486 has two positive and one negative eigenvalues (null of type B, see references in the previous paragraph). The three axes at the location of the null in Figs. 6 and 7 point in the direction of the three eigenvectors described in the previous section. The axis pointing approximately towards the solar south corresponds to the spine of the null (eigenvalue λ_3); while the other two axes define the fan plane, the one pointing approximately towards the solar west is the one with the lowest eigenvalue. This last eigenvalue is approximately twice lower than the other one. A study of the field structure in the vicinity of null points created by theoretical configurations similar to that of AR 10486 can be found in Mandrini et al. (2006). In the right panel of Fig. 6 we have computed field lines starting integration at finite distances from the null as described in the figure caption.
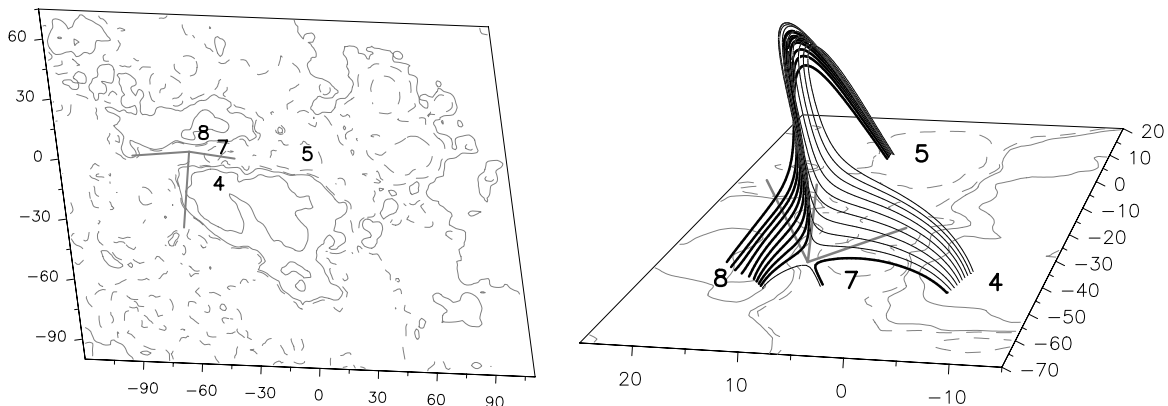

Fig. 6. The left panel shows the magnetic null point location in the coronal magnetic field of AR 10486. This figure represents the observer's point of view. The right panel depicts the null location from a different point of view. Field lines in this panel have been computed starting integration at finite distances from the coronal null. A set of thin continuous field lines follow roughly the direction of the eigenvector with the lowest eigenvalue in the fan plane. These have footpoints where polarities 4 and 5 lie. These field lines could reconnect at the null with field lines linking 7 to 8, these are represented by only one short and thin continuous line. After reconnection, we would have the set of thick continuous field lines that have footpoints at polarities 8 and 5, and those that connect polarities 4 and 7 (the latter is represented by only one thick short continuous field line). The three eigenvectors of the Jacobian field matrix have been depicted at the null location in both panels. The meaning of each of these axes is described in the text. The negative (positive) field isocontours are shown in continuous (dashed) thin lines, their values are ±100 G and ± 1000 G. The axes are labeled in Mm. Polarities are indicated in both panels.
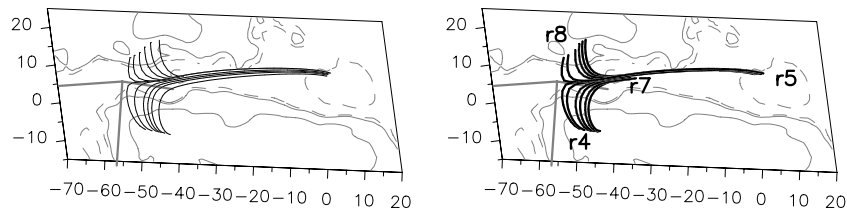
Fig. 7. Coronal magnetic field model of AR 10486 close to the magnetic null point. The left and right panels show the field lines drawn in the right panel of Fig. 6 in the observer's point of view. The left panel shows the two sets of field lines representing the pre-reconnected loops (thin continuous lines). The right panel corresponds to field lines after reconnection at the null point (thick continuous lines). Notice that the shape of these lines follows closely the shape of TRACE loops in 195 Å in Figs. 5. Several short field lines have been added as compared to the right panel of Fig. 6. The isocontours of the field are ±100 G and ±1000 G, drawn with continuous (dashed) lines for the positive (negative) values. The axes are labeled in Mm. The approximate locations of the ribbons for both flares are indicated in the right panel (see Fig. 3 and Fig. 4), we also depict the location of the null as in the left panel of Fig. 6.

If magnetic reconnection occurs at the magnetic null point shown in Fig. 6, we expect to see two compact bright ribbons at the intersections of the spine with the photosphere over the positive polarities 4 and 8, and two additional ones, having an elongated shape, over the negative region between them (the photospheric trace of the fan). Hα and TRACE observations at 1600 Å show a remarkable agreement with the model (see Figs. 3 and 4).

The above conclusion is reinforced when we draw the field lines in the right panel of Fig. 6 in the observer's point of view, as shown in Fig. 7. The left panel in this figure corresponds to field lines before reconnection, while the ones after reconnection are shown in the right panel. The shape of the latter set of field lines follows closely the shape of TRACE loops in 195 Å shown in Figs. 5. Combining the magnetic field evolution analysis (Section 2.2) with the computed coronal field topology, we conclude that the magnetic null appears in the corona as polarities 7 and 8 emerge and grow in the pre-existing field of polarities 4 and 5 (Fig. 2). Then, our results confirm that magnetic nulls are favorable regions for magnetic reconnection, which is driven by the local photospheric magnetic evolution.

A coronal null point was found at almost the same location on 28 October, 2003, by Mandrini et al. (2006). The null point height above the photosphere was 4.3 Mm on that day. The bright short loops observed by TRACE 1 h before the large X17 flare, and all along this event, had the same shape as the loops seen by TRACE in 195 Å in our case. Furthermore, ribbons were observed at the same location as the flare ribbons observed during the M flares analyzed in this paper. The just described ribbons and loops on 28 October correspond to a small event that accompanied the large X17 flare. No magnetic null point was found at this location or near by on 26 October, 2003, by Li et al. (2006) who studied the magnetic field topology of AR 10486 in relation with an X1.2 flare on that day. Therefore, our results combined with those of Mandrini et al. (2006) show that this null point is a stable topological structure which stays at least two days. Furthermore, Régnier and Fleck (2004) used a non-linear force-free field extrapolation of a magnetogram from the Imaging Vector Magnetograph on 27 October, and found a coronal magnetic null point at the same location. The magnetic data and the extrapolation method are different from ours, giving further support to the stability of this magnetic null point.

4. Conclusion

The presence of coronal magnetic nulls implies that the magnetic configuration has a complex topology which is favorable for magnetic reconnection to occur. That is why their existence has been theoretically invoked as necessary for reconnection. However, it has been shown in many examples that flares occur in more general topologies than those having null points, i.e. with quasi-separatrix layers (see the reviews by Démoulin, 2005, 2006).

We model the coronal field of AR 10486 using a linear force-free approach, taking the observed longitudinal photospheric field as boundary condition. Since the AR field is highly non-potential, the magnetic stress (α value) is set to the highest possible value for this type of computation. Using this model, we have found a magnetic null at the coronal level. It is located very low down in the corona, at a height of $\approx$3 Mm above the photosphere. Computing field lines starting at finite distances from the null, we are able to reproduce the special shapes for two sets of observed coronal loops for two M flares that occurred on 27 October, 2007. We conclude that these small loops were formed by magnetic reconnection during both homologous M flares. The correspondence between the computed field lines, located in the vicinity of a magnetic null, with the observed loops also validates our magnetic extrapolation.

A null point was also present at the same location one day later, on 28 October, 2003. Magnetic reconnection at this null point was at the origin of the small confined event that accompanied the large two-ribbon flare on that day (Mandrini et al., 2006). The existence of a null point at almost the same location, though at different coronal heights (a change due to the local photospheric evolution), demonstrates that this coronal null points is a stable topological structure. The origin of this stability is the presence of a quadrupolar region (polarities 4, 5, 7 and 8) which globally stays unchanged and defines the coronal magnetic

topology. The modification of the magnetic shear simply deforms this magnetic topology shifting slightly the location of the magnetic null and its separatrices.

Acknowledgements

References

Alissandrakis, C.E. On the computation of constant alpha force-free magnetic field. A&A 100, 197–200, 1981.

Antiochos, S.K., DeVore, C.R., Klimchuk, J.A. A model for solar coronal mass ejections. ApJ 510, 485–493, 1999.

Aulanier, G., DeLuca, E.E., Antiochos, S.K., McMullen, R.A., Golub, L. The topology and evolution of the bastille day flare. ApJ 540, 1126–1142, 2000.

Démoulin, P. Magnetic topologies: where will reconnection occur? in: Innes, D.E., Lagg, A., Solanki, S.A. (Eds.), ESA SP-596: Chromospheric and Coronal Magnetic Fields, 2005.

Démoulin, P. Extending the concept of separatrices to QSLs for magnetic reconnection. Advances in Space Research 37, 1269–1282, 2006.

Démoulin, P., Bagalá, L.G., Mandrini, C.H., Hénoux, J.C., Rovira, M.G. Quasi-separatrix layers in solar flares. II. Observed magnetic configurations. A&A 325, 305–317, 1997.

Démoulin, P., Hénoux, J.C., Mandrini, C.H. Are magnetic null points important in solar flares? A&A 285, 1023–1037, 1994.

Fernández Borda, R.A., Mininni, P.D., Mandrini, C.H., Gómez, D.O., Bauer, O.H., Rovira, M.G. Automatic solar flare detection using neural network techniques. Solar Physics 206, 347–357, 2002.

Fletcher, L., Metcalf, T.R., Alexander, D., Brown, D.S., Ryder, L.A. Evidence for the flare trigger site and three-dimensional reconnection in multiwavelength observations of a solar flare. ApJ 554, 451–463, 2001.

Gaizauskas, V., Mandrini, C.H., Démoulin, P., Luoni, M.L., Rovira, M.G. Interactions between nested sunspots II. A confined X1 flare in a delta-type sunspot. A&A 332, 353–366, 1998.

Gary, G.A., Moore, R.L. Eruption of a multiple-turn helical magnetic flux tube in a large flare: evidence for external and internal reconnection that fits the breakout model of solar magnetic eruptions. ApJ 611, 545–556, 2004.

Green, L.M., López Fuentes, M.C., Mandrini, C.H., Démoulin, P., van Driel-Gesztelyi, L., Culhane, J.L. The magnetic helicity budget of a CME-prolific active region. Solar Physics 208, 43–68, 2002.

Greene, J.M. Geometrical properties of three-dimensional reconnecting magnetic fields with nulls. JGR 93 (12), 8583–8590, 1988.

Handy, B.N., Acton, L.W., Kankelborg, C.C., Wolfson, C.J., Akin, D.J., Bruner, M.E., Caravalho, R., Catura, R.C., Chevalier, R., Duncan, D.W., Edwards, C.G., Feinstein, C.N., Freeland, S.L., Friedlaender, F.M., Hoffmann, C.H., Hurlburt, N.E., Jurcevich, B.K., Katz, N.L., Kelly, G.A., Lemen, J.R., Levay, M., Lindgren, R.W., Mathur, D.P., Meyer, S.B., Morrison, S.J., Morrison, M.D., Nightingale, R.W., Pope, T.P., Rehse, R.A., Schrijver, C.J., Shine, R.A., Shing, L., Strong, K.T., Tarbell, T.D., Title, A.M., Torgerson, D.D., Golub, L., Bookbinder, J.A., Caldwell, D., Cheimets, P.N., Davis, W.N., Deluca, E.E., McMullen, R.A., Warren, H.P., Amato, D., Fisher, R., Maldonado, H., Parkinson, C. The transition region and coronal explorer. Solar Physics 187, 229–260, 1999.

Lau, Y.T. Magnetic nulls and topology in a class of solar flare models. Solar Physics 148, 301–324, 1993.

Lau, Y.-T., Finn, J.M. Three-dimensional kinematic reconnection in the presence of field nulls and closed field lines. ApJ 350, 672–691, 1990.

Li, H., Schmieder, B., Aulanier, G., Berlicki, A. Is pre-eruptive null point reconnection required for triggering eruptions? Solar Physics 237, 85–100, 2006.

Longcope, D.W. Topological methods for the analysis of solar magnetic fields. Living Reviews in Solar Physics 2, 1–58, 2005.

Longcope, D.W., McKenzie, D., Cirtain, J., Scott, J. Observations of separator reconnection to an emerging active region. ApJ 630, 596–614, 2005.

Longcope, D.W., Silva, A.V.R. A current ribbon model for energy storage and release with application to the flare of 7 January 1992. Solar Physics 179, 349–377, 1998.

Luoni, M.L., Mandrini, C.H., Démoulin, P. Magnetic topology analysis of an M6 7. solar flare. Boletín de la Asociación Argentina de Astronomía La Plata Argentina 48, 84–87, 2005.

Mandrini, C.H., Démoulin, P., Hénoux, J.C., Machado, M.E. Evidence for the interaction of large scale magnetic structures in solar flares. A&A 250, 541–547, 1991.

Mandrini, C.H., Démoulin, P., Schmieder, B., Deluca, E., Pariat, E., Uddin, W. Companion event and precursor of the X17 flare on 28 October, 2003. Solar Physics 238, 293–312, 2006.

Mandrini, C.H., Démoulin, P., van Driel-Gesztelyi, L., Schmieder, B., Cauzzi, G., Hofmann, A. 3D Magnetic reconnection at an X-ray bright point. Solar Physics 168, 115–133, 1996.

Mandrini, C.H., Rovira, M.G., Démoulin, P., Hénoux, J.C., Machado, M.E., Wilkinson, L.K. Evidence for magnetic reconnection in large-scale magnetic structures in solar flares. A&A 272, 609–620, 1993.

Molodenskii, M.M., Syrovatskii, S.I. Magnetic fields of active regions and their zero points. Soviet Astronomy 21, 734–741, 1977.

Parker, E.N. Sweet's mechanism for merging magnetic fields in conducting fluids. JGR 62, 509–520, 1957.

Régnier, S., Fleck, B. Magnetic field evolution of AR 0486 before and after the X17 Flare on October 28, 2003. in: Walsh, R.W., Ireland, J., Danesy, D., Fleck, B. (Eds.), ESA SP-575: SOHO 15 Coronal Heating. pp. 519–522, 2004.

Scherrer, P.H., Bogart, R.S., Bush, R.I., Hoeksema, J.T., Kosovichev, A.G., Schou, J., Rosenberg, W., Springer, L., Tarbell, T.D., Title, A., Wolfson, C.J., Zayer, I.MDI Engineering Team The solar oscillations investigation - Michelson Doppler Imager. Solar Physics 162, 129–188, 1995.

Sweet, P.A. The neutral point theory of solar flares. In: IAU Symp. 6: Electromagnetic Phenomena in Cosmical Physics. p. 123, 1958.

Zhang, H.-Q., Bao, X.-M., Zhang, Y., Liu, J.-H., Bao, S.-D., Deng, Y.-Y., Li, W., Chen, J., Dun, J.-P., Su, J.-T., Guo, J., Wang, X.-F., Hu, K.-L., Lin, G.-H., Wang, D.-G. Three super active regions in the descending phase of solar cycle 23. Chinese Journal of Astronomy and Astrophysics 3, 491–494, 2003.